Radiation Damage Limitations in the Design of the Wisconsin Tokamak Fusion Reactor

G.L. Kulcinski, R.G. Brown, R.G. Lott, and P.A. Sanger

November 6, 1973

UWFDM-81

FUSION TECHNOLOGY INSTITUTE

UNIVERSITY OF WISCONSIN

MADISON WISCONSIN

Radiation Damage Limitations in the Design of the Wisconsin Tokamak Fusion Reactor

G.L. Kulcinski, R.G. Brown, R.G. Lott, and P.A. Sanger

Fusion Technology Institute
University of Wisconsin
1500 Engineering Drive
Madison, WI 53706

http://fti.neep.wisc.edu

November 6, 1973

UWFDM-81

(FDM 81)

RADIATION DAMAGE LIMITATIONS IN THE DESIGN OF THE WISCONSIN TOKAMAK FUSION REACTOR

MATERIALS

KEYWORDS: *fast neutrons, Tokamak devices, thermonuclear reactors, radiation effects, ductility, swelling, reactor materials, Type-316 stainless steel, elongation, embrittlement, voids, sputtering, erosion, thermonuclear reactor walls*

G. L. KULCINSKI, R. G. BROWN,* R. G. LOTT, and P. A. SANGER
University of Wisconsin, Nuclear Engineering Department
Madison, Wisconsin 53706

Received November 13, 1973
Revised December 11, 1973

A detailed analysis of the radiation damage problems to be expected in a specific D-T fueled fusion reactor has been conducted. The system examined is the 5000-MW(th) University of Wisconsin Tokamak reactor (UWMAK), which is constructed of 20% cold-worked Type-316 stainless steel and operated at a maximum temperature of 500°C and a neutron wall loading of 1.25 MW/m². The major radiation damage problem appears to be the loss in ductility; that is, the uniform elongation of the Type-316 stainless steel in the UWMAK-I first wall may fall to <0.5% after one to two years of operation. Another serious problem will be the void-induced swelling in the steel. Based on current design equations, the swelling in the steel of the first wall will exceed the design limit of 10% in approximately five years of operation. The wall erosion rate due to neutron and charged-particle sputtering, coupled with exfoliation due to blistering, is calculated to be 0.22 mm/yr. Finally, calculations reveal that the radiation damage problems in the superconducting magnets can be incorporated into the design without difficulty. The integral wall-loading limits for embrittlement, swelling, wall erosion, and magnet damage in UWMAK are calculated to be 2, 6, 25, and 100 MW yr/m², respectively.

INTRODUCTION

It is not an exaggeration to state that the structural materials of a D-T fusion reactor, and in particular those in the first wall facing the plasma, will be subjected to the most intense radiation environment ever produced by man. Each 14-MeV neutron will cause tens of thousands of displaced atoms as it slows down to thermal energy. Most of the displaced atoms (>99.99%) will rearrange themselves on the other lattice sites, so it might appear that no long lasting damage would remain. However, if just a few hundredths of a percent of the atoms do not regain a suitable lattice position, the metal can be severely damaged. This damage will degrade the mechanical and physical properties of most materials to the point that they must be frequently replaced *or* the power level of the reactor must be lowered to uneconomical levels.

The purpose of this paper is to summarize the problems that are expected to occur in a specific D-T fueled fusion power plant, the University of Wisconsin Tokamak Design (UWMAK) described in Refs. 1 and 2. We have chosen to confine our remarks to the specific materials in that reactor for three reasons. First, the environmental parameters for the structural components are quantitatively defined throughout the reactor (i.e., neutron and charged particle energy spectrum, temperature, stresses, etc.). Second, it was felt that by focusing on specific materials which are likely candidates for early-generation fusion power plants (e.g., Type-316 stainless steel), we would be able to point out where current data are applicable and where future data may be required. Finally, we hope to emphasize the relative effect that each of the damage mechanisms will have on limiting the allowable neutron wall loading in the reactor.

DESCRIPTION OF THE UWMAK-I REACTOR

The fusion reactor described here was designed with the philosophy that there would be as little extrapolation of present-day technology as pos-

*Present address: Westinghouse Advanced Reactors Division, Madison, Pennsylvania 15663.

sible. Such an approach produced a rather conservative design compared to what may be ultimately possible for fusion reactors far into the twenty-first century. However, we feel that the system as presently designed could be constructed with a minimum of technological development after thermonuclear plasma confinement has been demonstrated. This conservative approach should be borne in mind when examining the UWMAK-I efficiencies, structural design, and magnet construction.

The basic parameters of UWMAK-I are summarized in Table I and described in more detail in Refs. 1 and 2. The reactor is a Tokamak system utilizing a double-null poloidal divertor. A cross section of the reactor is shown in Fig. 1. UWMAK-I has been sized by optimizing the cost per unit power in a β-limited system where the costs are assumed to scale as the magnet costs. Inputs to the optimization are the power level of 5000 MW(th) and a neutron wall loading of 1.25 MW/m^2; the former was chosen because prelimi-

TABLE I

Basic Characteristics of UWMAK-I

Power	5000 MW(th) [1500 MW(e)]
Major radius	13 m
Minor radius	5 m
Divertor	poloidal, double-null
Temperature	$T_i = T_e = 11$ keV
Density	$\bar{n}_i = 8 \times 10^{13}$ cm^{-3}
Coolant	lithium
Structural material	Type-316 stainless steel
Neutron wall loading	1.25 MW/m^2
Magnetic field	3.8 T (on axis) 8.66 T (max)
Magnets	superconducting niobium-titanium cryogenically stabilized with copper
Power cycle	lithium-steam

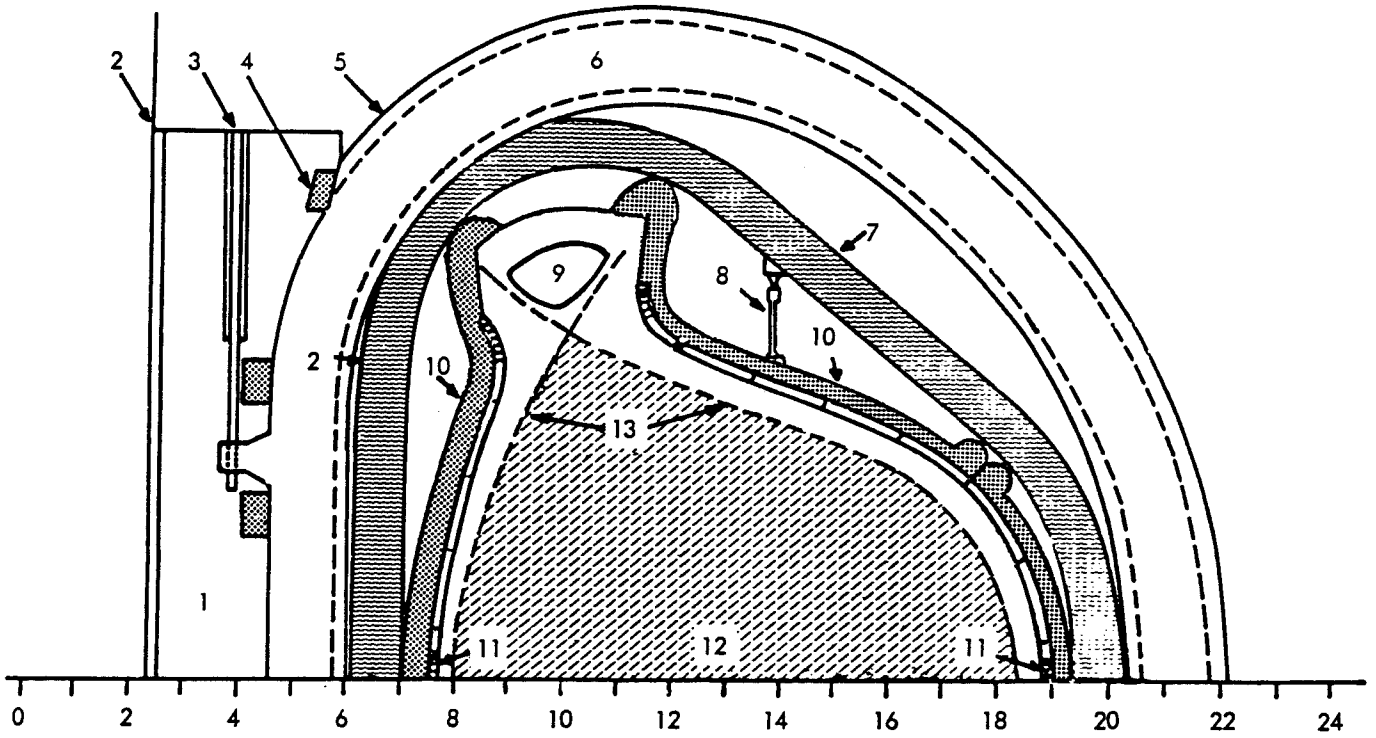

Fig. 1. Schematic view of UWMAK-I fusion reactor:

1. central core (stainless steel)
2. superinsulation (Mylar)
3. magnet support shear pins
4. transformer coils (Nb-Ti + Cu)
5. toroidal magnet Dewar (stainless steel)
6. toroidal magnet (Nb-Ti + Cu)
7. shield (Pb + B_4C + SS)
8. blanket support
9. vacuum port shield
10. reflector and poloidal header
11. heat removal cells
12. plasma
13. separatrix.

nary studies indicated that the benefit of going to larger systems was minimal, and the latter because of radiation damage considerations, the topic of this paper. Constraints imposed by the space requirements of an air-core transformer with superconducting windings have also been included. A more detailed description of the plasma-operating conditions and divertor principles are given in Ref. 1.

The main toroidal field magnets are superconducting using niobium-titanium filaments cryogenically stabilized with copper. The maximum field in the magnets is 86.6 kG at 4.2°K, and the field on the plasma axis is 38 kG. To minimize the peak stresses and the amount of structural material needed, the "D" shape of the magnets in Fig. 1 has been determined by detailed stress calculations.

The blanket and shield of UWMAK-I are shown schematically in Fig. 2, while the primary characteristics are listed in Table II. The coolant, moderator, and breeding material is lithium. The low exit temperature (483°C) of the lithium is dictated by the corrosion rate of the structural material (Type-316 stainless steel) by lithium. At this temperature, 1500 to 2500 kg of metallic corrosion products must be removed from the primary lithium circuit per year to avoid plugging the heat exchanger and also to avoid high radioactivity levels in the maintenance areas (Ref. 3). The total power required to pump the lithium is 22 MW(e), which is 1.5% of the plant output. This low value has been achieved by design techniques that reduce the average coolant velocity and avoid excessive eddy-current losses. The structural material (20% cold-worked Type-316 stainless steel) has been chosen because of the established industrial capabilities with this material and the

TABLE II

Blanket and Shield Characteristics

Blanket thickness	73.4 cm
Vacuum-gap thickness	1.0 cm
Shield thickness	77.0 cm
Blanket coolant	lithium
inlet pressure	400 psig
inlet temperature	283°C
outlet temperature	483°C
pumping power	22 MW(e)
Structure	Type-316 stainless steel (20% cold-worked)
maximum temperature	500°C
maximum stress	914 kg/cm² (13 000 psi)
corrosion rate	1500 to 2500 kg/yr
First-wall lifetime	2 yr
neutron wall loading	1.25 MW/m²
heat load	12.5 W/cm³
Shield coolant	helium, 51.7 kg/cm² (50 atm) 200°C

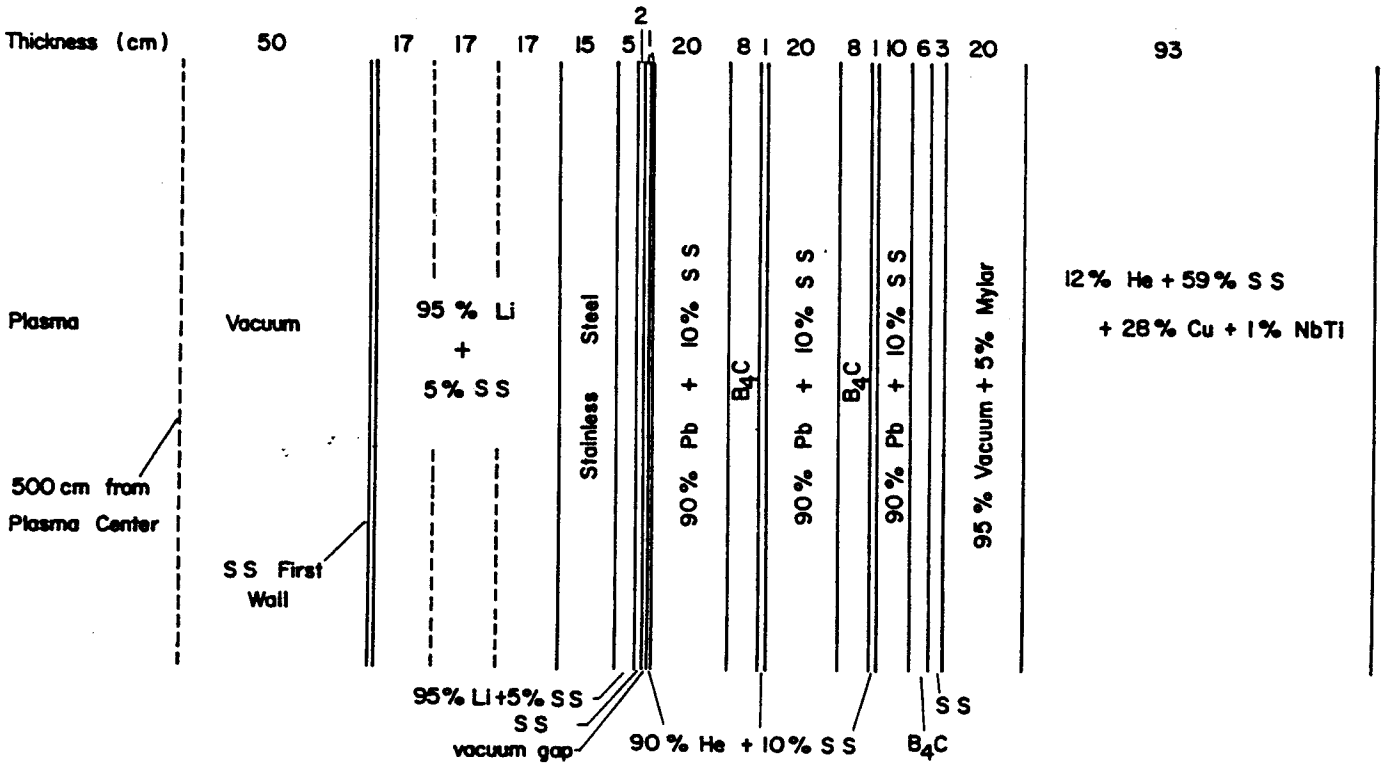

Fig. 2. Schematic of UWMAK-I blanket, shield, and magnet structure.

wealth of data available on thermal, mechanical, chemical, neutronic, and physical properties in both liquid-metal and irradiation environments. A 1-cm vacuum gap is used between the blanket and shield to aid in dropping the temperature from 500 to 200°C. The shield is helium gas cooled and consists of layers of B_4C and lead; the former material is used to slow down and absorb neutrons and the latter to absorb the high gamma-ray flux from the blanket. The total heat generated in the shield is 50 MW(th).

Neutron and photon transport calculations give a breeding ratio of 1.49, which implies a doubling time on the order of two to three months.[1] The tritium breeding is likely to be adequate for all uncertainties in nuclear data or design. Detailed heating calculations, based on kerma factors from the MACK program, were performed and reveal that 16.55 MeV of energy is produced per incident 14.06-MeV neutron. Thus, the total energy per fusion event, including the 3.52-MeV alpha-particle energy is 20.07 MeV. This is in contrast to values of 22 to 27 MeV which have commonly been used in computing power output for fusion plants.

The effect of transmutation reactions on the properties of Type-316 stainless steel is given in Ref. 4, as are the secondary effects of the nuclear reactions in the structural material—radioactivity and afterheat.

TABLE III

Summary of Radiation Damage Environment at the UWMAK-I First Wall

Particle	Energy (keV)	Flux (cm^2/sec)
Deuterium	23	6.4×10^{13}
Tritium	23	6.4×10^{13}
Helium	23	4.7×10^{12}
Helium	23 to 3500	1.7×10^{11}
Neutrons	14.1 MeV (current)	5.5×10^{13}
Neutrons[a]	$0.1 < E < 14.1$ MeV	3.3×10^{14}
Metal ions	23	2.5×10^{12}

[a]Total neutrons, excluding current.

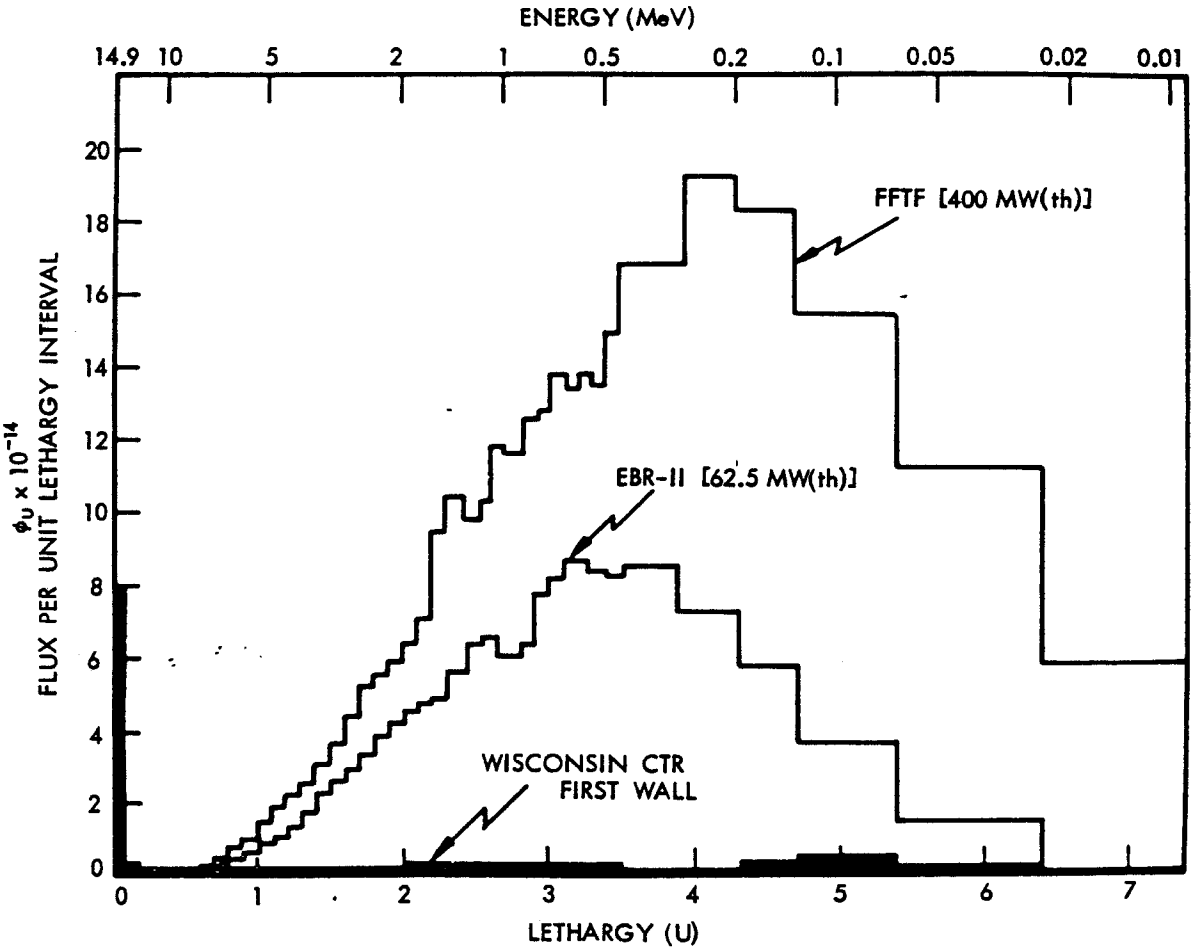

Fig. 3. Comparison of calculated neutron spectra for UWMAK-I [5000-MW(th)] fusion reactor to EBR-II and FFTF fission reactors.

RADIATION ENVIRONMENT IN UWMAK

A summary of the irradiation conditions at the first wall in UWMAK-I is given in Table III. The charged-particle fluxes have been obtained assuming a 90% efficient divertor. The neutron spectrum for the first wall is shown in Fig. 3. For comparison, the neutron spectra of two fission reactors, the Fast Flux Test Facility (FFTF) and Experimental Breeder Reactor-II (EBR-II), are also included in Fig. 3.

Note that the charged-particle flux to the first wall consists mainly of D+ and T+ with a smaller level of thermalized helium atoms and an even smaller flux of metal atoms which have been sputtered from the first wall, diffused into the plasma, gained energy, and then have been returned to the first wall by normal diffusion processes. The total neutron flux [$\sim 3.9 \times 10^{14}$ n/(cm^2 sec)] is smaller than that normally found in a fission reactor, but the higher average energy of the neutrons in UWMAK tends to produce more damage per neutron. The absolute damage rate will be about the same in both types of reactors.

The general scheme used to calculate the displacement cross sections for Type-316 stainless steel is described elsewhere,[5,6] and only a brief account is given here. Neutron interactions treated explicitly were elastic scattering, inelastic-scattering (n,n'), $(n,2n)$ reactions, and (n,γ) reactions. The (n,γ) reaction was included because it is the sole source of displaced atoms at neutron energies below several hundred eV. Other reactions such as (n,α) and (n,p) were neglected at this time in calculating displacement cross sections; their contribution at 14 MeV is estimated to be <15% for the stainless steel, and at lower energies their contribution is negligible.

The four mechanisms listed above produce primary knock-on atoms (PKAs) that, in turn, lose their energy by electronic excitation or by nuclear energy transfers to surrounding atoms. This latter form of energy transfer causes further displacements. The total displacement cross section at energy E is just

$$F(E) = F_{el}(E) + F_{inel}(E) + F_{(n,2n)}(E) + F_{(n,\gamma)}(E) \quad , \tag{1}$$

where

$F_{el}(E)$ = displacement cross section due to elastic scattering, isotropic at low energies (<0.1 MeV) and anisotropic at higher energies

$F_{inel}(E)$ = displacement cross section due to inelastic scattering with anisotropy being taken into account in the case of iron

$F_{(n,2n)}(E)$ = displacement cross section due to $(n,2n)$ reactions

$F_{(n,\gamma)}(E)$ = displacement cross section due to the energetic recoils which result from (n,γ) reactions (mainly from low-energy neutrons).

The general expression for $F(E)$ is

$$F(E) = \sigma(E) \int_{E_d}^{T_{max}} p(E,T)\,dT \quad , \tag{2}$$

where

$\sigma(E)$ = appropriate interaction cross section

$p(E,T)$ = probability that a neutron of energy E transfers energy T to the PKA

$\nu(T)$ = number of displacements produced by a PKA with energy T

E_d = energy required to displace an atom.

The problem then is twofold: (a) to determine $p(E,T)$ and hence the number and energy spectrum of the PKAs, and (b) to choose a model to calculate the average number of atoms displaced by each PKA of energy T. The choice of $p(E,T)$ has been reviewed elsewhere.[5] The evaluation of $\nu(T)$ is essentially independent of the type of scattering that produced the PKA, and we will briefly consider this problem.

The results for this study are based on the Lindhard et al. theory[7] of slowing down of energetic atoms in solids. Lindhard et al. have derived from the Thomas-Fermi theory a function of $L(\epsilon)$, the kinetic energy (in dimensionless form) that is transferred to the atoms of a cascade initiated by a PKA having initial dimensionless energy ϵ; that is, the fraction of PKA energy available to cause displacements in $L(\epsilon)/\epsilon$, while the remainder is lost in electron excitation. It has recently been suggested that this fraction be reduced by 20% to account for deviation from hard sphere interactions.[8] In the present work, the number of displacements per PKA was taken to be

$$\nu(T) = \frac{\beta L(\epsilon)}{\epsilon} \frac{T}{2E_d} \quad , \tag{3}$$

where $\beta = 0.8$. For a material of atomic number Z and atomic weight A,[a] Lindhard et al. give

$$L(\epsilon) = \epsilon \left[1 + K_L g(\epsilon)\right]^{-1} \quad , \tag{4}$$

where

$$\epsilon = A_L T$$

[a] Weighted averages were used for stainless steel; the assumed composition was 18% Cr and 10% Ni by weight. The results are insensitive to small changes of composition.

$$A_L = (0.01151)\,(Z)^{-7/3}\ \text{eV}^{-1}$$

$$K_L = 0.1337\,(Z)^{2/3}\,A^{-1/2}\ .$$

The convenient numerical approximation to $g(\epsilon)$ given by Robinson[9] was used here, namely,

$$g(\epsilon) = \epsilon + 0.40244\,\epsilon^{3/4} + 3.4008\,\epsilon^{1/6}\ .$$

It has been recently decided[8,10] that the standard value of E_d for steel should be 40 eV. This is somewhat higher than the threshold displacement energy of 24 eV (Ref. 11) and qualitatively it represents a value averaged over all the directions of displacement in the crystal structure. For stainless steel, Eq. (3) then becomes

$$\nu(T) \cong 10\,\frac{L(\epsilon)T}{\epsilon}\ (\text{keV})\ , \qquad (5)$$

The principal source of scattering cross-section data was the Evaluated Nuclear Data File, Version III (ENDF/B-III) (Ref. 12), for chromium (MAT 1121) and nickel (MAT 1123). In the regions of resonance elastic scattering, BNL-325 (Ref. 13) was also used for chromium and nickel.

ENDF/B data (MAT 1124), obtained in pointwise form from the Oak Ridge Radiation Shielding Information Center, were used for iron. These data were subsequently modified slightly[10] primarily by raising a prominent trough at ~24 keV—for inclusion in ENDF/B-III under a new number, MAT 1180. The differences between the two evaluations are believed to be insignificant for present purposes.

The (n,γ) cross sections are proportional to $1/\sqrt{E}$ over most of the energy range of interest. With the exception of iron, BNL-325 data[13] were used in the resonance regions. Because of incomplete knowledge of the gamma-ray emission process, the estimates of the (n,γ) contributions to the displacement cross sections are more uncertain than for the other processes. For neutron energies above several keV, the (n,γ) contribution is negligible in comparison with other contributions. On the other hand, for neutrons with energies below that required to displace an atom in an elastic encounter—ranging from ~300 to ~900 eV for metals considered here—the (n,γ) reaction is the principal source of displacement events.

The displacement cross sections used for this work are given in Table IV, and some typical displacement rates are shown in Fig. 4. These displacement rates were calculated for the typical heat removal cell shown in Fig. 4. The lithium enters the cell at 283°C and flows perpendicularly to the plasma in a "zig-zag" motion, continually picking up heat until it reaches a temperature of 483°C at the outlet. The temperature along the first wall varies from 300 to 500°C and the damage

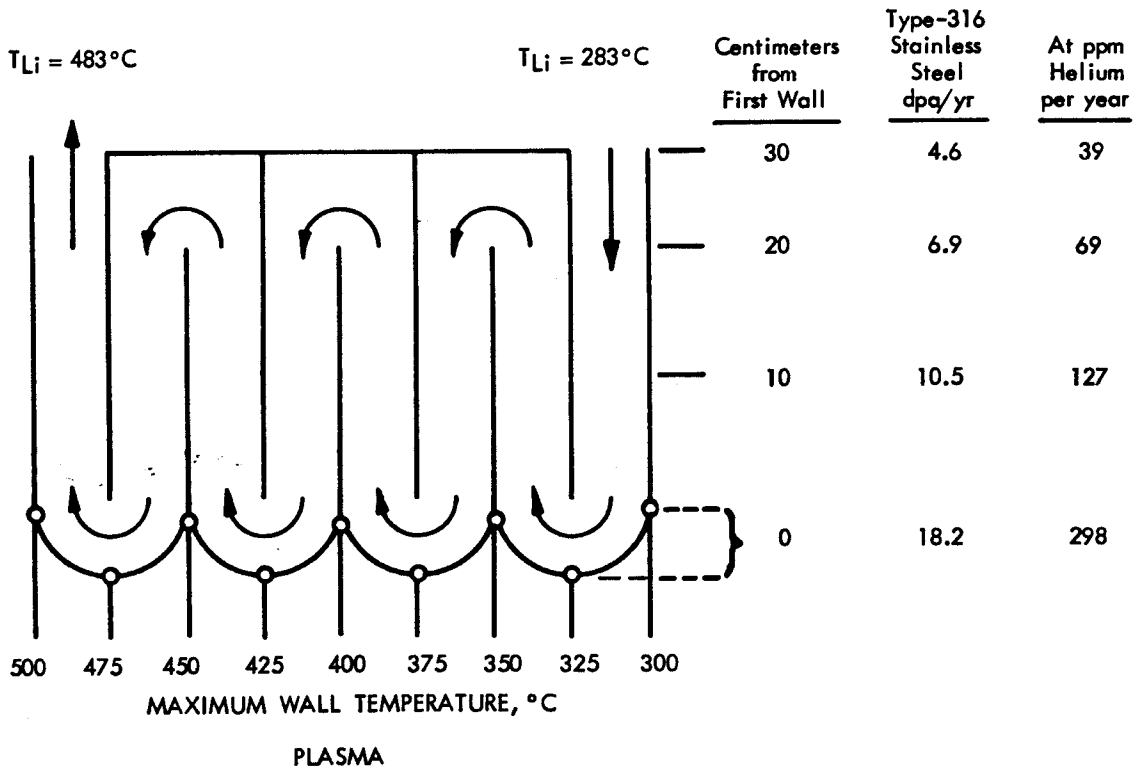

Fig. 4. Spatial distribution of temperature and radiation damage rates in UWMAK-I.

rates vary from 18.2 displacements per atom (dpa) per year at the first wall to 4.6 dpa/yr at 30 cm into the blanket.

The gas production rate via (n,α) and (n,p) reactions has also been calculated as a function of distance into the blanket. The reaction cross sections were processed by MACK (Ref. 14) and then multiplied by the neutron spectrum at various positions throughout the blanket.[15] It is seen in Fig. 4 that almost 300 appm of helium is produced per year in the first wall [including the contributions from impurities and ^{59}Ni (see Ref. 4)] and this drops to ~39 appm/yr at 30 cm from the first wall. The hydrogen production drops by a similar amount from 636 appm/yr at the first wall to 118 appm at a distance of 30 cm into the blanket.

EMBRITTLEMENT IN UWMAK BLANKET COMPONENTS

Perhaps the most dramatic effect of neutron irradiation on Type-316 stainless steel is the reduction of its ductility. There are three primary ways in which this ductility loss can be measured: (a) total elongation at failure, (b) reduction of area at failure, and (c) uniform elongation (ϵ_u). We have chosen the latter because of the ease with which it can be applied to engineering analysis.

There appear to be two mechanisms by which irradiation lowers ϵ_u—helium embrittlement and matrix hardening.[16-19] Helium embrittlement results from the generation of helium gas within the matrix by (n,α) reactions and the collection of the helium gas bubbles at grain boundaries. These bubbles can grow under the action of applied stress by diffusional properties until the grain boundaries fail. Ultimately, the bubbles may lead to failure by assisting crack nucleation at second-phase particles within the boundaries.

Matrix hardening can lead to premature failure by forcing most of the deformation to be absorbed by the grain boundaries. Such an effect results in excessive grain-boundary shearing, which leads to high stresses and subsequent failure initiated at grain-boundary triple points.

It is extremely important to note that when helium is present at boundaries and irradiation hardening is significant, the helium embrittlement and matrix hardening can *combine* to produce ductility losses more severe than the two processes acting alone.[18] Under such conditions, strain is concentrated at the grain boundaries which, because of helium embrittlement, are less able to withstand shear than before irradiation. These result in grain-boundary failure at much smaller strains than simple matrix hardening alone.

The general temperature region for pure helium embrittlement is found to be >600°C and that for pure matrix hardening between 500 and 600°C; matrix hardening and helium embrittlement can combine to cause a reduction in ϵ_u as described above. Since the maximum wall temperature in UWMAK-I is <500°C, we will assume that most of the ductility loss is due to matrix hardening and that current fast-reactor data can be used. This approach ignores the helium which is produced at a relatively high rate in a Controlled Thermonuclear Reactor (CTR). Note that this approach would not be reasonable for structural temperatures of 550°C or greater.

Experimental information on the value of ϵ_u for irradiated solution-treated Type-316 stainless steel is shown in Fig. 5 (Refs. 20 through 26). The data are plotted in terms of displacements per atom on the basis of 47 dpa per 10^{23} n/cm^2 ($E >$ 0.1 MeV). The striking feature of Fig. 5 is that it would predict extremely low values of ϵ_u (<1%) after 10 to 20 dpa in the 426 to 650°C temperature range. We have coupled the information in Fig. 5 with the dpa-temperature information in Fig. 4 to

TABLE IV

Displacement Cross Sections for Type-316 Stainless Steel [$(E_d)_{eff}$ = 40 eV]

Lower Energy (MeV)	Cross Section (barns)	Lower Energy (MeV)	Cross Section (barns)	Lower Energy (eV)	Cross Section (barns)
13.50	2220	0.4505	366	1234	3.18
12.21	2080	0.4076	415	961.1	5.76
11.05	1990	0.3688	423	748.5	1.96
10.00	1950	0.3337	244	582.9	1.58
9.048	1910	0.3020	224	457.3	1.20
8.187	1900	0.2752	199	353.6	0.126
7.408	1900	0.2472	197	275.4	0.127
6.703	1850	0.2237	193	214.5	0.143
6.065	1760	0.2024	180	167.0	0.159
5.488	1700	0.1832	240	130.1	0.179
4.966	1660	0.1657	174	101.3	0.203
4.493	1620	0.1500	161	78.89	0.228
4.066	1560	0.1357	222	61.44	0.256
3.679	1490	0.1228	161	47.65	0.289
3.329	1410	0.1111	89.8	37.27	0.328
3.012	1380	0.08652	128	29.02	0.371
2.725	1300	0.06738	147	22.60	0.421
2.466	1270	0.05247	74.5	17.60	0.477
2.231	1170	0.04087	71.0	13.71	0.541
2.019	1050	0.03183	67.1	10.68	0.616
1.827	997	0.02479	190	8.315	0.689
1.653	824	0.01930	17.9	6.476	0.779
1.496	790	0.01503	29.9	5.043	0.884
1.353	758	0.01171	29.0	3.928	0.999
1.225	727	(ev)	(barns)	3.059	1.13
1.225	649			2.382	1.28
1.003	516	9119	18.9	1.855	1.46
0.9072	459	7102	31.6	1.445	1.67
0.8208	435	5531	20.2	1.125	1.91
0.7427	511	4307	15.4	0.8764	2.11
0.674	489	3355	11.3	0.6826	2.37
0.6081	382	2613	7.21	0.5316	2.70
0.5502	313	2035	5.08	0.4140	3.06
0.4979	349	1585	2.92	0.0220	5.31

predict the behavior of Type-316 stainless steel in the UWMAK-I blanket. The results are listed as a function of distance from the wall, temperature, and irradiation time in Table V and are displayed in Fig. 6.

We have rather arbitrarily (and perhaps conservatively) chosen 0.5% uniform elongation as the lower design limit in UWMAK-I. This value may have to be adjusted upward because of the large number of startup and shutdown operations required in UWMAK-I (~20/day).

It can be seen from Table V that after one year of irradiation only the first few centimeters of the blanket will have reached the 0.5% elongation limit. However, within the next year the ductility of the first 20 cm of the blanket will fall below that limit. In fact, within two years of irradiation the entire heat removal cell structure will have uniform elongation values of <0.5%.

A rather disturbing feature of Fig. 6 is the fact that even the Type-316 stainless steel in the header region behind the heat removal cells will fall below the ductility limit after ten years of irradiation. Within 30 years, the projected lifetime of the plant, we find that the entire blanket structure will be below or close to the design limit.

The conclusion of this work is that somewhere between one and two years of irradiation one will have to remove the heat removal cells (the first 20 cm of the UWMAK blanket) and replace them with new units. Strictly speaking, the units should be changed every year, but it is felt that the lifetime may be extended to two years because of some uncertainties in the data.

It is quite apparent that if one is to retain any reasonable ability to absorb the stress and strains imposed on the blanket by startup, shutdown, or those due to swelling and coolant pressures, one must begin to think in terms of replaceable first walls! Once this concept can be mastered, the frequency of change (one or two years) becomes a matter of economics.

One last point should be emphasized—the problem of replacing the headers and reflectors in the blanket. The data in Fig. 6 indicate that the header region should be replaced every ten years and the reflectors after 15 to 20 years. Such a possibility will greatly increase the amount of radioactive stainless steel which must be disposed of because there is approximately ten times more steel in the reflector region than in the heat cells and because the headers contain about twice the amount of steel as do the heat cells.

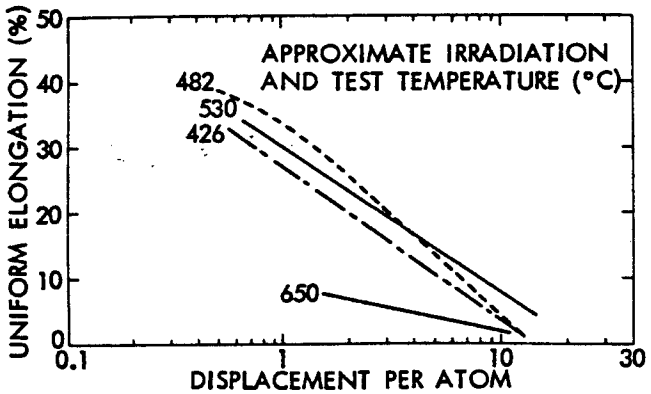

Fig. 5. Effect of displacement damage on the uniform ductility of solution-treated Type-316 stainless steel (Refs. 20 through 26).

SWELLING PROBLEMS IN UWMAK-I

The production of voids in austenitic stainless steel was first discovered in 1966 (Ref. 27), and since that time these alloys have been studied in great detail. The general reasons why voids form in metals are fairly well understood, and several theories for void growth have been proposed in the past few years.[28-30] The reader is referred to several recent conferences for a full view of this phenomenon.[31-34]

Recent theoretical analysis by Brailsford and Bullough[28] predicts that the swelling in steel can be described by the following equation:

$$\frac{\Delta V}{V_o} = K(t - t_o)S_o F \quad , \qquad (6)$$

where

K = defect production rate

Kt_o = incubation dose required for void formation

S_o = term which includes material parameters, such as the dislocation density, sink density, and precipitate density

TABLE V

Anticipated Ductility Changes in UWMAK-I Structure Material (Type-316 stainless steel)

Distance from First Wall (cm)	Temperature (°C)	Damage Level (dpa/yr)	Uniform Elongation Remaining (%)			
			1 yr	2 yr	10 yr	30 yr
0	300 to 426	18.2	<0.5	<0.5	<0.5	<0.5
0	426 to 500	18.2	<0.5	<0.5	<0.5	<0.5
10	300 to 426	10.5	4	<0.5	<0.5	<0.5
10	426 to 500	10.5	5	<0.5	<0.5	<0.5
20	300 to 426	6.9	7	~0.5	<0.5	<0.5
20	426 to 500	6.9	9	~0.5	<0.5	<0.5
30	300 to 426	4.6	11	4	<0.5	<0.5
30	426 to 500	4.6	15	8	<0.5	<0.5
40	300 to 426	3.2	15	8	<0.5	<0.5
50	300 to 426	2.2	20	12	<0.5	<0.5
60	300 to 426	0.87	27	19	5	<0.5
70	300 to 426	0.45	35	27	12	~0.5

F = function of temperature.

The important features of Eq. (6) and the Brailsford and Bullough theory[28] are that swelling appears to increase linearly with damage, that the magnitude of swelling is inversely proportional to the dislocation density and coherent precipitate density, and that the swelling is very low below ~0.3 and above ~0.5, the absolute melting point.

Empirical formulas for the fluence and temperature dependence of swelling in Type-316 stainless steel have also been developed.[35] The form of these equations for solution-treated and cold-worked Type-316 stainless steel are shown in Fig. 7. The solution-treated Type-316 stainless steel swells more than the cold-worked Type-316 stainless steel at a given temperature and fluence in accordance with recent theories, and the temperature dependence is qualitatively the same as predicted by Brailsford and Bullough.[28]

The swelling expected in the UWMAK-I blanket as a function of distance from the first wall, temperature, and irradiation time is given in Table VI for both solution-treated and 20% cold-worked Type-316 stainless steel. It is obvious that the cold-worked alloy shows much more resistance to swelling than does the annealed alloy. For example, the maximum swelling at the first wall

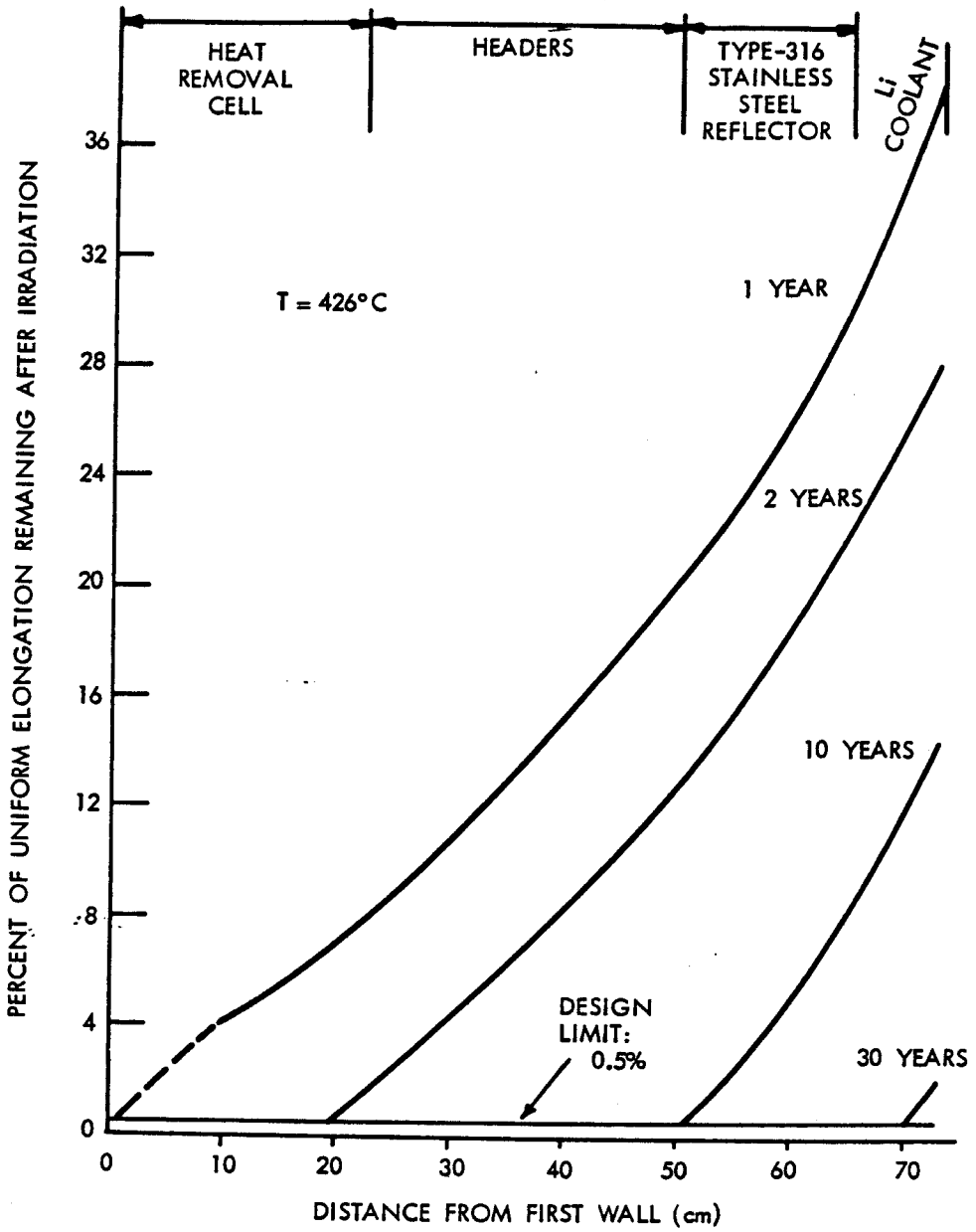

Fig. 6. Anticipated uniform elongation remaining in Type-316 stainless steel after irradiation in UWMAK-I.

after two years is ~7.9% for solution-treated Type-316 stainless steel and only 0.25% for the cold-worked Type-316 stainless steel. This difference is somewhat less after ten years of irradiation, but if a 10% maximum swelling limit is placed on UWMAK-I components, it is quite apparent that the limit will be reached sooner by the solution-treated alloy.

The anticipated maximum swelling for 20% cold-worked Type-316 stainless steel is plotted in Fig. 8 as a function of distance and irradiation time. Note that after ten years of irradiation, swelling values of 10% or more will be found in the first 10 cm of the blanket. If the blanket were not replaced during the 30-yr lifetime, it is apparent that more than 40 cm of the blanket could exceed the design limit and that the maximum swelling near the first wall could be exceedingly high, ~80 to 90%.

It is also clear that even if one uses one of the more swelling-resistant alloys now known, cold-worked Type-316 stainless steel, wall replacement will still be required about every seven years. One should also recognize that the embrittlement and swelling limits are not completely independent. Swelling gradients can impose severe stress gradients and large strains in rigidly fastened components. If these swelling-induced strains exceed the allowed values, premature failure could occur.

SURFACE PROBLEMS IN UWMAK-I

The first wall of the UWMAK reactor will be subjected to intense fluxes of high-energy ions during operation. These particles can cause a multitude of surface disruptions,[36] but the two most important are sputtering and blistering.

Sputtering occurs when a metallic target is bombarded by high-energy ions, neutrons, or neutral atoms and when these particles displace atoms in the target from their lattice sites. Not all of these displaced atoms remain in the target. They may be sputtered off the front surface of the target and ejected from the back surface. Several theoretical studies on sputtering have been devel-

TABLE VI

Summary of Anticipated Swelling Behavior of Type-316 Stainless Steel in UWMAK-I

Distance from First Wall (cm)	Temperature (°C)	Damage Level (dpa/yr)	% $\Delta V/V_0$					
			2 yr		10 yr		30 yr	
			Solution Treated	20% Cold Worked	Solution Treated	20% Cold Worked	Solution Treated	20% Cold Worked
0	300	18.2	0.42	<0.1	1.5	<0.1	3.0	<0.1
0	325	18.2	0.51	<0.10	1.7	<0.1	4.0	0.1
0	350	18.2	0.59	<0.1	2.1	0.2	5.0	0.65
0	375	18.2	0.75	<0.1	3.2	0.8	8.6	2.5
0	400	18.2	1.2	0.14	7.6	2.4	26	7.5
0	425	18.2	2.2	0.19	28	6.2	>100[a]	21
0	450	18.2	4.8	0.24	>100[a]	10	>100[a]	34
0	475	18.2	7.1	0.24	>100[a]	17.5	>100[a]	57
0	500	18.2	7.9	0.25	>100[a]	25	>100[a]	80
10	325	10.5	0.38	<0.1	1.1	<0.1	2.6	<0.1
10	375	10.5	0.61	<0.1	2.0	<0.1	5.3	1.4
10	425	10.5	0.99	<0.1	12	2.5	65	8.5
10	475	10.5	2.3	<0.1	69	8	>100[a]	30
10	500	10.5	2.4	<0.1	87	13	>100[a]	48
20	325	6.9	0.26	<0.1	0.82	<0.1	1.8	<0.1
20	375	6.9	0.4	<0.1	1.3	0.25	3.8	0.9
20	425	6.9	0.55	<0.1	6.0	1.4	34	7.3
20	475	6.9	0.51	<0.1	28	4.5	>100[a]	20
20	500	6.9	1.0	<0.1	35	6.7	>100[a]	29
30	325	4.6	0.19	<0.1	0.6	<0.1	1.3	<0.1
30	375	4.6	0.22	<0.1	0.9	0.13	2.4	0.6
30	425	4.6	0.31	<0.1	3.3	0.58	16	4.2
30	475	4.6	0.38	<0.1	16	1.6	>100[a]	13
30	500	4.6	0.36	<0.1	14	3.6	>100[a]	18
40	500	3.2	0.15	<0.1	6.2	0.38	80	11
50	500	2.2	<0.1	<0.1	2.5	<0.1	30	5.8
60	500	0.87	<0.1	<0.1	0.36	<0.1	3.8	<0.1

[a]Values not considered reliable.

oped,[37] and good reviews of the theory are presented elsewhere.[36,38]

Irradiation of metal surfaces with energetic charged particles not only causes atoms to be sputtered from the first wall, but it can also cause severe surface roughening and blistering.[39-43] Qualitatively, the energetic ions (only hydrogen and helium isotopes will be considered here) displace atoms as they penetrate the solid. When they lose most of their energy, they slow down and become trapped because of their low diffusivity. Since the solubility of some gases in metals (e.g., helium) is extremely small, most of the gas precipitates into small bubbles. These small bubbles are formed in a region near the end of the range for the gas atom. This region also corresponds to that for maximum vacancy production. The bubbles can capture these vacancies, grow, and eventually coalesce with other bubbles to form lenticular bubbles below the surface of the metal. If enough atoms are injected at an elevated temperature, the pressure in these bubbles will be high enough to deform the metal surface, causing it to protrude above the original surface. Eventually, this "blister" can rupture, causing a large flake of the wall material to be spalled off.

The erosion rate due to sputtering and blistering by many types of species may be calculated by

$$\frac{\Delta l}{t} = \sum_{\mu} S_{\mu} \phi_{\mu} \frac{A_w}{N_o \rho} \quad , \qquad (7)$$

where

Δl = thickness of wall removed

S_{μ} = yield in atoms removed from the wall per particle for a particular bombarding particle μ

ϕ_{μ} = flux of the bombarding particle μ

A_w = atomic weight of the material

t = irradiation time

N_o = Avogadro's number

ρ = density of the wall material.

The method of calculating S is described elsewhere,[1] and Table VII lists the values used for this study.

TABLE VII

Summary of First-Wall Erosion Rates in UWMAK-I

Ion	Mean Energy (keV)	S	Flux (cm²/sec)	Erosion Rates (mm/yr)	% Total[a]
Sputtering					
D+	23	0.02	6.4×10^{13}	0.0047	2
T+	23	0.03	6.4×10^{13}	0.0070	3
He	23	0.15	4.7×10^{12}	0.0026	1
He	~100	0.03	1.7×10^{11}	0.00002	-
n	>10 000	0.2	9.4×10^{13}	0.14[b]	64
n	0.1 to 10 000	0.009	3.4×10^{14}	0.022[b]	10
Metal	23	2.5	2.6×10^{12}	0.023	10
			Total Sputtering	~0.20	
Blistering					
He	23	1	4.7×10^{12}	0.017	8
He	~100	3	1.7×10^{11}	0.0019	1
D+	23	0.01	6.4×10^{13}	0.0023	1
T+	23	0.01	6.4×10^{13}	0.0023	1
			Total Blistering	~0.024	

Total Wall Erosion Rate ~0.22 mm/yr

[a]Will not total 100% due to roundoff.

[b]Include both sides of wall.

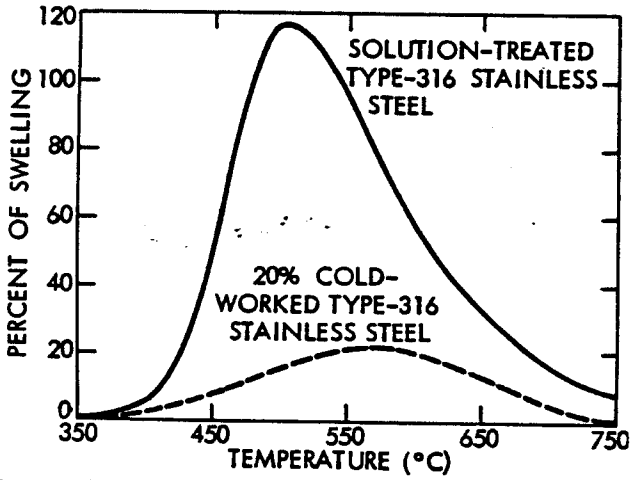

Fig. 7. Predicted swelling for solution-treated and 20% cold-worked stainless steel (Ref. 35) irradiated to 118 dpa.

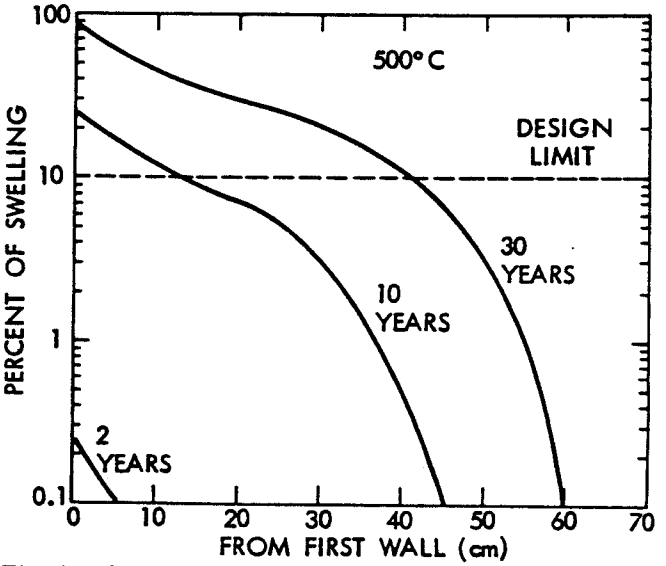

Fig. 8. Anticipated maximum swelling for 20% cold-worked Type-316 stainless steel in UWMAK-I blanket.

The sputtering values for deuterium and tritium were estimated from Ref. 36 and the value for 23-keV helium from data of McCracken and Erents.[44] The sputtering yield for 100-keV helium was estimated using the theory of Pease,[37] while the 14.1-MeV neutron sputtering yield comes from recent experiments by Kaminsky[45] on cold-worked niobium. The value for lower energy neutrons comes from the suggested value for niobium[45] and the relative values of Garber et al.[46] Finally, the self-ion sputtering coefficient is estimated from data on 45-keV iron ions[36] and data over a range of energies for copper.[47]

The effective removal coefficient for blistering comes from recent work by Das and Kaminsky[48] on Type-304 stainless steel, and this has been adjusted for lower energy helium by the ratio of the particle ranges. Finally, the (D + T) blistering rates were assumed to be 1/100 of the helium blistering rates; this is due to their higher diffusivity, higher threshold for blister formation in steel,[43] and inhomogeneous blister formation.

The amount of material removed from the first wall as a function of irradiation time is shown in Fig. 9 and listed in Table VII. The first point to note is that two-thirds of the total wall erosion rate (0.22 mm/yr) is due to the 14-MeV neutrons, and almost three-fourths is due to sputtering by neutrons of all energies. The next important contributor to wall erosion comes from the self-ion bombardment, and this amounts to ~10% of the total. Blistering only accounts for 11% of the erosion rate, while all the other charged-particle sputtering produces <6%.

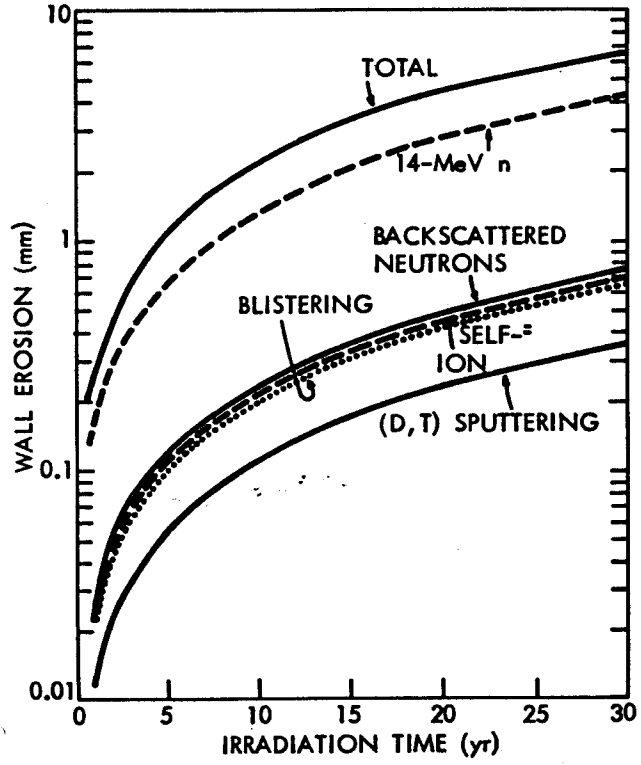

Fig. 9. Anticipated particle erosion of UWMAK-I Type-316 stainless-steel first wall.

Note that if there were no divertor at all, the total wall erosion rate would increase only by a factor of 3 to 4 over short time periods. Clearly, if no catastrophic self-ion buildup occurs, one could operate the first wall at the increased wall erosion rate for a few years. However, if we wish to limit the wall erosion due to particle bombardment to <1 mm (the maximum Δl allowed by stress in Type-316 stainless steel is ~3.3 mm, including corrosion loss), then there is a six-year limit at UWMAK-I operating conditions.

RADIATION DAMAGE TO SUPERCONDUCTING MAGNETS

The potential damage to the magnet components can be divided into two major categories[1]: (a) reduction in J_c of the superconductor, niobium-titanium, and (b) increased resistance of the copper stabilizer. Analysis has shown that the displacement rate at the magnet surface is on the order of 6×10^{-5} dpa/yr or 1.8×10^{-3} dpa/30 yr. Soell, Wipf, and Vogl[49] have shown that at $\sim 2 \times 10^{-3}$ dpa there would be less than 10% reduction in J_c of niobium-titanium at 4.2°K. Since it appears that this reduction in J_c could be easily tolerated in UWMAK-I with only slight modifications to the conductor design, radiation damage of the niobium-titanium filaments is not a limiting feature of this reactor.

The stabilizing material in the magnet—copper—was chosen primarily for its low resistivity. It is well known that irradiation at low temperature (~4.2°K) produces defects that have extremely low mobility and tend to increase the resistivity of any metal.[50] Such an effect is particularly evident in high-purity materials.

The rate of resistivity increase of copper at low temperatures has been given by Horak and Blewitt[51] as

$$\frac{d\rho_r}{dt} = A(1 - B\rho_r)^2 \quad , \qquad (8)$$

where

ρ_r = radiation-induced resistivity component

A, B = constants.

The saturation resistivity $\rho_{r\infty}$ for copper is 0.33×10^{-6} Ω-cm, and the saturation defect concentration is 1.3×10^{-3} dpa. A plot of the resistivity of copper during neutron irradiation is presented in

Fig. 10. Note that very little effect is observed below 5×10^{-5} dpa (approximately one year of UWMAK-I irradiation).

The present design follows the conservative total stability criterion first suggested by Stekly, Thome, and Strauss.[52] This criterion states that the cooling of the conductor by the helium must be greater than the amount of heat generated by the total current flowing in the stabilizer. This criterion presupposes that the current is forced to leave the superconductor for one reason or another. Stated mathematically,

$$I^2 \frac{\rho_T \cdot l}{Wh} \leq qWl \quad , \tag{9}$$

where

I = conductor current, A

ρ_T = total resistivity, Ω-cm

q = heat flux, W/cm^2

W = cooling surface width, cm

h = conductor thickness, cm

l = total conductor length.

The total resistivity is comprised of the intrinsic resistivity ρ_o, the magnetoresistivity ρ_m, and the radiation-induced resistivity ρ_r which is a function of time. The magnet is designed such that the current is the same at all times; this means that

$$I^2 = \frac{qW^2h}{\rho_o + \rho_m} = \frac{q(W + \Delta)^2h}{\rho_o + \rho_m + \rho_r} \quad , \tag{10}$$

where the radiation-induced resistivity has been accommodated by the additional conductor width Δ. Solving for Δ/W yields

$$\frac{\Delta}{W} = \left(1 + \frac{\rho_r}{\rho_o + \rho_m}\right)^{1/2} - 1 \quad . \tag{11}$$

Both ρ_r and ρ_m are functions of distance into the magnet, and an expression for the conductor width as a function of position in the magnet can be obtained using the following relationships for ρ_r and ρ_m:

$$\rho_r = \rho_{r\infty}\left[\frac{\text{dpa}(0)\exp\left(-\frac{x}{\lambda}\right)}{\text{dpa}(0)\exp\left(-\frac{x}{\lambda}\right) + C_{d\infty}}\right] \quad . \tag{12}$$

$$\rho_m = 0.455\, B_{\max}\left(1 - \frac{x}{t}\right) \quad , \tag{13}$$

where

x = distance from inner most conductor turn

dpa(0) = highest damage level in the magnet at $x = 0$

t = thickness of magnet windings

λ = displacement decay constant (~12.5 cm)

$B_{\max}$ = maximum magnetic field, T.

This formulation permits the radiation damage to be accounted for within the conductor design. This additional width as a function of the depth into the magnet is shown in Fig. 11. Note that this modification drops from 20% to <3% within the first 30 cm of the magnet, based on the dpa damage after one year of operation and a maximum field of 8.7 T. The length of the time between room-temperature anneals has to be determined by the economic balance of the additional cost of copper versus the 60 days of reactor downtime necessary for the annealing procedure. Assuming a 90% recovery per warmup,[50] one can calculate the thickness increase of the stabilizer to keep the same I^2R losses in irradiated copper; this is plotted in Fig. 12. Note that the requirement for a 20% increase in material goes up to 100% when the magnet warmup is extended from every year to every ten years.

It is not possible to put a rigid wall-loading limit on this effect as it is mostly economic in nature and would require much more detailed cost analysis than is presently available for UWMAK-I.

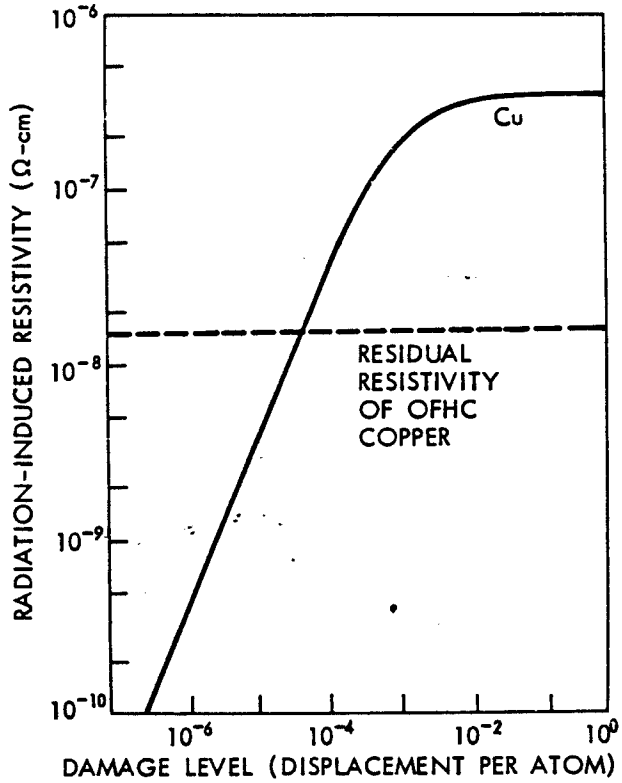

Fig. 10. Anticipated radiation-induced resistivity increase of copper stabilizer in UWMAK-I magnet.

However, it is not possible to accommodate more than a 100% increase of the copper stabilizer for mechanical reasons; if the magnets are warmed up every two years during the replacement of the first wall, this would imply a neutron wall-loading limit of 6.3 MW/m^2. If one allows a factor of 2 for the fact that perhaps ~10% of the damage does not anneal completely at room temperature, then the above wall loading implies an integral limit of ~100 MW-yr/m^2.

SUMMARY

From the discussion in this paper, it is clear that the major barrier to increasing the wall loading in UWMAK-I is the loss of ductility due to displacement damage. A convenient way to state this limitation is in terms of MW-yr/m^2. Table VIII summarizes the values calculated in this paper.

The loss of ductility limits the integral wall loading to ~2 MW-yr/m^2; that is, one expects the walls would have to be replaced after one to two years at a 1.25-MW/m^2 wall loading. If one had wanted the wall to last for the full 30-yr lifetime, the reactor would have to operate at ~0.06 MW/m^2. Clearly, such an operating point is uneconomical.[1]

It now appears that the integral wall-loading limitation on the first wall is due to void swelling in 20% cold-worked Type-316 stainless steel is ~6 MW-yr/m^2. Such a limitation implies that the first wall could survive a 0.2-MW/m^2 neutron wall loading for 30 years. This low value again appears to be uneconomical.

It is possible to get some appreciation for the benefits of using the cold-worked steel over the solution-treated alloy by comparing the integral wall-loading limitations for both metallurgical treatments. If one wants to limit the void swelling to <10%, then the solution-treated Type-316 stainless steel should be subjected to no more than 3.3 MW-yr/m^2 in UWMAK-I. This means that if embrittlement did not limit the wall lifetime to one to two years, swelling in solution-treated Type-316 stainless steel would limit it to two to three years. The use of cold-worked Type-316 stainless steel raises the possible lifetime due to swelling effect along to approximately five years.

The third major limitation is due to erosion of the first wall. It was discovered that if the most pessimistic sputtering and blistering rates are assumed and if the total wall thickness that can be eroded is ~3.3 mm, then the integral wall-loading

TABLE VIII

Summary of Integral Wall-Loading Limitations in UWMAK-I

Property	Design Limit	Wall-Loading Limit (MW-yr/m^2)
Embrittlement	ϵ_u >0.5%	~2
Swelling[a]	$\Delta V/V_0$ <10%	6
Wall erosion	Δl <3mm	~~15~~ 18
Copper resistivity increase	Inner winding thickness increase, <100%	~100

[a]For 20% cold-worked Type-316 stainless steel.

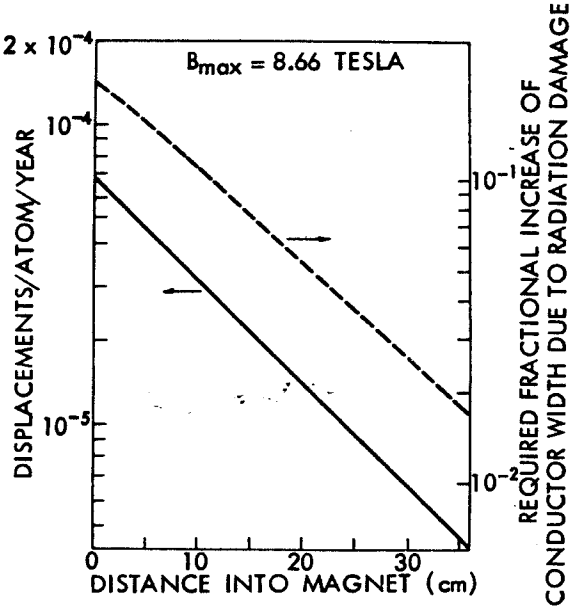

Fig. 11. Spatial distribution of displacement damage in UWMAK-I magnet and the required increase in stabilizer thickness required to keep the total current constant in UWMAK-I toroidal magnets.

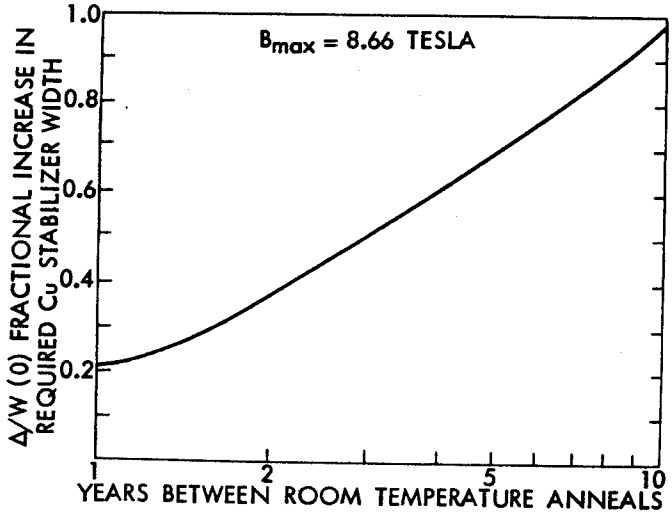

Fig. 12. The effect of periodic room-temperature anneals on the required thickness increase in copper stabilizer in UWMAK-I magnets.

limitation is ~18 MW-yr/m^2. (The exact value depends on the time because of the loss of material due to corrosion.) It appears that if no other limitations are placed on the first wall, then a 30-yr operation at 0.8 MW/m^2 would be marginally economic. However, if the high 14-MeV neutron sputtering rates of Kaminsky[45] are not substantiated in future experiments for Type-316 stainless steel, then the integral wall-loading limitation may be as much as 50 MW-yr/m^2.

Note that the major limitation in the toroidal magnet is due to the increase in resistivity of the copper stabilizer. The integral wall-loading limit resulting from this phenomenon is ~100 MW-yr/m^2. However, this can be extended by a factor of 2 simply by warming the magnets up to room temperature once a year instead of every other year.

Finally, it is necessary to end this paper on a note of caution. This analysis has been conducted with *theoretical* calculations of the damage state, temperature, and stress levels in the materials of a *hypothetical* reactor. We have used data from fission-reactor experiments where the helium production rates are a factor of 20 less than in fusion systems and we have used the most pessimistic values of property changes in Type-316 stainless steel to arrive at our conclusion. We feel that they are qualitatively correct, but the quantitative values should only be interpreted as reasonable estimates. Obviously, much more work is needed to fill in the data gaps, especially in the area of embrittlement of Type-316 stainless steel with high helium content (several thousand appm). We hope that this work will stimulate further detailed studies of alternate materials in other specific fusion-reactor designs.

REFERENCES

1. "Wisconsin Tokamak Reactor Design," University of Wisconsin Fusion Design Memo-68 (1973).

2. G. A. EMMERT, R. W. CONN, and G. L. KULCINSKI, "The Wisconsin Tokamak Reactor Design—An Overview," *Proc. Conf. 5th Symp. Engineering Problems of Fusion Research* (to be published).

3. A. B. JOHNSON and W. F. VOGELSANG, "An Assessment of Corrosion Product Transport Problems in a CTR," to be published in *Nucl. Technol.*

4. W. F. VOGELSANG, G. L. KULCINSKI, R. G. LOTT, and T. Y. SUNG, "Transmutations, Radioactivity, and Afterheat in a D-T Tokamak Reactor," to be published in *Nucl. Technol.*

5. D. G. DORAN, "Neutron Displacement Cross Sections for Stainless Steel and Tantalum Based on a Lindhard Model," *Nucl. Sci. Eng.*, **49**, 130 (1972).

6. G. L. KULCINSKI, D. G. DORAN, and M. A. ABDOU, "Displacement and Gas Production Rates in Candidate CTR Structural Materials," UWFDM-15, University of Wisconsin (1973).

7. J. LINDHARD, V. NIELSEN, M. SCHARFF, and P. V. THOMSEN, "Integral Equations Governing Radiation Effects," *Mat. Fys., Medd. Dan. Vid. Selsk.*, **33**, *10* (1963).

8. IAEA Specialists Meeting on Radiation Damage Units for Ferritic and Stainless Steels, October 31-November 1, 1972, Seattle, Washington.

9. M. T. ROBINSON, "The Energy Dependence of Neutron Radiation Damage in Solids," *BNES Conf. Nuclear Fusion Reactors*, p. 364, United Kingdom Atomic Energy Authority, Culham Laboratory (1969).

10. D. G. DORAN, unpublished results (1973).

11. P. G. LUCASSON and R. M. WALKER, "Production and Recovery of Electron Induced Radiation Damage in a Number of Metals," *Phys. Rev.*, **127**, 485 (1962).

12. H. C. HONECK, "ENDF/B—Specifications for an Evaluated Nuclear Data File for Reactor Applications," BNL-50066, Battelle-Northwest Laboratories (1966).

13. M. D. GOLDBERG, S. F. MUGHABGHAB, S. N. PUROHIT, B. A. MAGURNO, and V. M. MAY, "Neutron Cross Sections," 2nd ed., Suppl. 2, BNL-325, Brookhaven National Laboratory (1966).

14. M. A. ABDOU, C. W. MAYNARD, and R. Q. WRIGHT, "MACK: A Computer Program to Calculate Neutron Energy Release Parameters," ORNL-TM-3994, Oak Ridge National Laboratory (1973).

15. We are indebted to M. A. Abdou for calculating the neutron spectrum for UWMAK-I.

16. A. L. WARD and J. J. HOLMES, "Ductility Loss in Fast Reactor Irradiated Stainless Steel," *Nucl. Appl. Technol.*, **9**, 771 (1970).

17. J. J. HOLMES, A. J. LOVELL, and R. L. FISH, "Ductility of Irradiated Type-316 Stainless Steel," *Effects of Radiation on Substructure and Mechanical Properties of Metals and Alloys*, ASTM-STP-529, American Society for Testing and Materials (1973).

18. R. L. FISH and J. J. HOLMES, "Tensile Properties of Annealed Type-316 Stainless Steel After EBR-II Irradiation," *J. Nucl. Mater.*, **46**, 113 (1973).

19. R. L. FISH, A. J. LOVELL, H. R. BRAGER, and J. J. HOLMES, "Tensile and Creep Behavior of Cold Worked Type-316 Stainless Steel After EBR-II Irradiation," *Irradiation Embrittlement and Creep in Fuel Cladding and Core Components*, p. 187, British Nuclear Energy Society (1973).

20. P. SOO and J. McANDREW, WARD-3045T2C-3, Westinghouse Advanced Reactors Division (1972).

21. J. R. HAWTHORNE, NRL Memorandum Report 2088 (AD-703617), p. 7, Naval Radiation Laboratory (1970).

22. J. R. HAWTHORNE, "True Stress—Natural Strain Determination for High Temperature Alloys Exposed in EBR-II," WHAN-FR-40-1, p. 641, Hanford Engineering Development Laboratory (1971).

23. T. T. CLAUDSON, R. W. BARKER, and R. L. FISH, "The Effects of Fast Flux Irradiation on the Mechanical Properties and Dimensional Stability of Stainless Steel," *Nucl. Appl. Technol.*, **9**, 10 (1970).

24. J. O. STIEGLER and E. E. BLOOM, "Some Effects of Composition and Microstructures on Radiation Damage in Stainless Steels," ORNL-TM-3550, p. 90, Oak Ridge National Laboratory (1971).

25. M. M. PAXTON and F. R. SCHOBER, "Mechanical Properties of Irradiated 316 Stainless Steel," HEDL-71-176, Hanford Engineering Development Laboratory (1971).

26. A. L. WARD, L. D. BLACKBURN, and A. J. LOVELL, "Mechanical Properties of Fast Reactor Austenitic Stainless Steel Weldment Materials," *Trans. Am. Nucl. Soc.*, **14**, 556 (1971).

27. C. CAWTHORNE and E. J. FULTON, "Voids in Irradiated Stainless Steel," *Nature*, **216**, 575 (1966).

28. A. D. BRAILSFORD and R. BULLOUGH, "The Rate Theory of Swelling Due to Void Growth in Irradiated Metals," *J. Nucl. Mater.*, **44**, 121 (1972).

29. S. D. HARKNESS and CHE-YU LIE, "Theoretical Study of the Swelling of Fast Neutron Irradiated Material," *Proc. Intern. Conf. Radiation Induced Voids in Metals*, J. W. CORBETT and L. C. IANNIELLO, Eds., AEC Symposium Series 26, CONF-710601, p. 798, U.S. Atomic Energy Commission (1972).

30. H. WIEDERSICH, "On the Theory of Void Formation During Irradiation," *Rad. Effects*, **12**, 111 (1972).

31. *Proc. BNES European Conf. Voids Formed by Irradiation of Reactor Materials*, S. F. PUGH, Ed. (1971).

32. *Proc. Intern. Conf. Radiation Induced Voids in Metals*, J. W. CORBETT and L. C. IANNIELLO, Eds., AEC Symposium Series 26, CONF-710601, U. S. Atomic Energy Commission (1972).

33. *Proc. ASTM Conf. Effects of Radiation on Substructure and Mechanical Properties of Metals and Alloys*, ASTM-STP-529, American Society for Testing and Materials (1973).

34. *Proc. Intern. Conf. Defects and Defect Clusters in B.C.C. Metals and Their Alloys*, R. J. ARSENAULT, Ed., *Nucl. Met.*, **18** (1973).

35. J. J. LAIDLER, Hanford Engineering Development Laboratory, Richland, Washington, Private Communication (1973).

36. M. KAMINSKY, *Atomic and Ionic Phenomena on Metal Surfaces*, Academic Press, New York (1965).

37. R. S. PEASE, *Rend. SIF, Corso*, **13**, 158 (1959).

38. G. CARTER and J. COLLIGON, *Ion Bombardment of Solids*, American Elsevier Publishing Co., New York (1968).

39. M. KAMINSKY, *Proc. Intern. Working Session Fusion Reactor Technology*, CONF-710624, p. 86, U.S. Atomic Energy Commission (1971).

40. M. KAMINSKY and S. K. DAS, "Effect of Channeling and Irradiation Temperature on the Morphology of Blisters in Niobium," *Appl. Phys. Letters*, **21**, 443 (1972).

41. M. KAMINSKY and S. K. DAS, "Blistering of Polycrystalline and Monocrystalline Niobium," *Rad. Effects*, **18**, 245 (1973).

42. W. BAUER and G. J. THOMAS, "Helium Re-Emission and Surface Deformation in 316 SS During -170°C to 700°C Implantations," *Rad. Effects*, **18**, 245 (1973).

43. H. VERBEEK and W. ECKSTEIN, "Radiation Blistering after Hydrogen Ion Implantation into Surfaces of Stainless Steel and Molybdenum," *Proc. Conf. Applications of Ion Beams to Metals*, to be published.

44. G. M. McCRACKEN and S. K. ERENTS, "Ion Burial in the Divertor of a Fusion Reactor," *Proc. BNES Conf. Nuclear Fusion Reactors*, p. 353, United Kingdom Atomic Energy Authority, Culham Laboratory (1969).

45. M. KAMINSKY, Private Communication (1973).

46. R. I. GARBER et al., "Radiation Sputtering and Damage of Certain Metals in the Radiation Field of a Nuclear Reactor," *Atomnaya Energiya*, **28**, 400 (1970).

47. O. E. ALMÉN and G. BRUCE, "Sputtering Experiments in the High Energy Region," *Nucl. Instr. Methods*, **11**, 279 (1961).

48. S. K. DAS and M. KAMINSKY, to be published.

49. M. SOELL, S. L. WIPF, and G. VOGL, "Change in Critical Current of Superconducting NbTi by Neutron Irradiation," *Proc. Conf. Applied Superconductivity*, p. 434 (1972).

50. J. W. CORBETT, *Advances in Solid State Physics*, Suppl. 7, Academic Press, New York (1965).

51. J. A. HORAK and T. H. BLEWITT, "Fast Neutron Irradiation Induced Resistivity in Metals," *Phys. Stat. Sol.*, **9**, 721 (1972).

52. Z. J. J. STEKLY, R. THOME, and B. STRAUSS, "Principles of Stability in Cooled Superconducting Magnets," *Proc. Summer Study Superconducting Devices and Accelerators*, BNL 50155 (C-55), p. 748, Brookhaven National Laboratory (1968).